Biosensors and Bioelectronics 40 (2013) 422–426

Contents lists available at SciVerse ScienceDirect

Biosensors and Bioelectronics

journal homepage: www.elsevier.com/locate/bios

Short communication

Electrochemical impedance spectroscopy biosensor with interdigitated electrode for detection of human immunoglobulin A

Ryuzo Ohno [a], Hitoshi Ohnuki [a,*], Huihui Wang [a], Takuya Yokoyama [a], Hideaki Endo [b], Daiju Tsuya [c], Mitsuru Izumi [a]

[a] Division of Marine Technology, Tokyo University of Marine Science and Technology, 2-1-6 Etchujima, Koto-ku, Tokyo 135-8533, Japan
[b] Division of Marine Science, Tokyo University of Marine Science and Technology, 4-5-7 Konan, Minato-ku, Tokyo 108-8477, Japan
[c] National Institute for Materials Science, 1-2-1 Sengen, Tsukuba, Ibaraki 305-0047, Japan

ARTICLE INFO

Available online 10 August 2012

Keywords:
Electrochemical impedance spectroscopy
Interdigitated microelectrode
Immunosensor
Human immunoglobulin A

ABSTRACT

Interdigitated electrodes (IDEs) that have a series of parallel microband electrodes with alternating microbands connected together were utilized in electrochemical impedance spectroscopy (EIS) to build a label-free human immunoglobulin A (IgA) immunosensor. Anti-human IgA (anti-IgA) was employed as an IgA receptor and was covalently immobilized on the IDE surface through a self-assembled monolayer, as confirmed by atomic force microscopy. EIS measurements revealed that the specific adsorption of IgA onto the immobilized anti-IgA gave rise to a clear increase in the value of interfacial charge transfer resistance (R_{ct}). A linear relationship between ΔR_{ct} and the logarithm of IgA concentration was found for the concentration range of 0.01–100 ng/mL. No modulation of R_{ct} was detected by immersing the sensor in solutions of other proteins such as human immunoglobulin G or bovine serum albumin, which confirmed a high selectivity of this immunosensor for IgA. These results demonstrated that the anti-IgA receptor simply immobilized on the IDE surface can provide a sensitive biosensor.

1. Introduction

The concentration of immunoglobulins in blood is known to be a good indicator of a variety of diseases (Kutukculer et al., 2007). Consequently, accurately monitoring of the immunoglobulin concentration in blood allows for early detection of these diseases. The antigen–antibody reaction, which is a selective binding interaction between specific antigen and antibody pairs, provides a sensing principle of the immunoglobulin sensor. However, the antigen–antibody reaction is difficult to detect as it is a simple molecular adsorption process, which unlike enzymatic reactions, does not generate a final detectable product. Accordingly, labeled methods such as the ELISA method have been generally used in diagnosis and in laboratory examinations (Gosling, 1997). ELISA, however, requires a high degree of skill to operate, and also takes time and effort, which makes it difficult for non-specialists to apply for point-of-care diagnostics (Lequin, 2005). On the other hand, EIS detects antibody–antigen reactions as electrical signals directly and does not need a labeling process or other pretreatment process. The easy and rapid detection aspect of EIS promises the application of easy diagnosis (Daniels and Pourmand, 2007). EIS analyzes the resistance and capacitance that occurs at the electrode surface, which are very sensitive to biological binding events. This feature makes EIS suitable for measuring antigen–antibody reactions. To date, several immunosensors based on EIS have been developed (Lisdat and Schäfer, 2008; Qi et al., 2010).

In recent years, significant progress in nanoproduction technologies such as photo- or electron-beam lithography or micromachining techniques has opened up new opportunities for assembling electrochemical analyzing systems (Laschi and Mascini, 2006). The technology allows the fabrication of IDEs that have a series of parallel microband electrodes, in which the alternating microbands are connected together. The IDE structure offers many promising advantages such as a fast establishment of a steady-state, a high sensitivity, a large aspect ratio, and a great signal-to-noise ratio (Niwa et al., 1990). Because of the short distance between the anodic and cathodic electrodes, the speed of the oxidation and reduction cycle is extremely enhanced, which results in a high efficiency of data collection. Furthermore, the effective surface area of an IDE is larger than that of conventional electrodes, which enables an increased sensitivity of the sensor. A common application of IDEs to the EIS technique is as a faradic EIS that uses the redox probe, $[Fe(CN)_6]^{3-/4-}$. Besides the abovementioned advantages, the employment of IDEs in faradic EIS eliminates the need for a reference electrode. Such a simple two electrode system is favorable for the mass production of chip-type sensors, since all the electrodes

* Corresponding author. Tel./fax: +81 3 5245 7466.
E-mail address: ohnuki@kaiyodai.ac.jp (H. Ohnuki).

0956-5663/$ - see front matter © 2012 Elsevier B.V. All rights reserved.
http://dx.doi.org/10.1016/j.bios.2012.07.052

can be patterned with the same material. To date, many kinds of EIS biosensor employing the IDE structure have been reported: immunosensors (Arya et al., 2010), DNA sensors (Li et al., 2006), affinity sensors using aptamer probes (Xu et al., 2005), biosensors for bacterial cells (Yang et al., 2004; Varshney and Li, 2009) and viruses (Wang et al., 2009).

In this paper, we describe a label-free EIS immunosensor using IDEs for highly sensitive detection of human IgA. To our knowledge, this is the first IgA immunosensor employing EIS with an IDE structure. The antibody to IgA (anti-IgA) was employed as a molecular recognition element and covalently immobilized on the IDE surface through the use of a self-assembled monolayer (SAM). Atomic force microscopy (AFM) measurements were performed to confirm the absorption of IgA to the IDE surface. The characteristic feature of our sensor is the very simple surface structure: the molecular receptor of anti-IgA was simply anchored on the surface without any modifications by CNT or metal nanoparticles. Since EIS is a very sensitive method to the surface condition, its sensitive nature results in potential drawbacks. Bogomolova et al. reported that the surface conditions can be changed very easily by the redox probe in solution, an applied voltage, and even by incubation in a buffer (Bogomolova et al., 2009). Thus we considered that the simple surface structure would be more stable than a modified surface. In this report, we fabricated an IDE based biosensor with the simple surface structure and characterized its sensing performance.

2. Experimental

2.1. Chemicals

3-mercaptopropionic-acid (MPA), 1-ethyl-3-carbodiimide hydrochloride (EDC), *N*-hydroxysuccinimide (NHS), IgA, human immunoglobulin G (IgG), bovine serum albumin (BSA), and anti-IgA were purchased from Sigma-Aldrich. Phosphate-buffered saline (PBS, 50 mM, pH 7.4, 6.0 and 4.0) was prepared by adding 3.0 g NaH_2PO_4 and 3.55 g Na_2HPO_4 in 500 mL of deionized water. Then, the pH of the PBS was adjusted with 50 mM NaOH or H_3PO_4. Both IgA and IgG solutions were prepared in PBS at pH 6.0.

2.2. Fabrication of IDEs

IDEs were fabricated on a quartz glass plate (1 cm × 2 cm × 0.05 cm, Daico, Japan) using photolithography techniques. Ti/Au (400/2000 Å) layers were deposited on the SiO_2 surface of the quartz plate and were patterned through lift-off process. The Au IDEs with 130 fingers of 8 mm length and 20 μm width, separated with a 20 μm gap between adjacent fingers were patterned on the plate.

2.3. Preparation of SAM modified electrodes

The substrate was pretreated in piranha solution (3:1 mixture of H_2SO_4 and H_2O_2) for 10 min and then rinsed in deionized

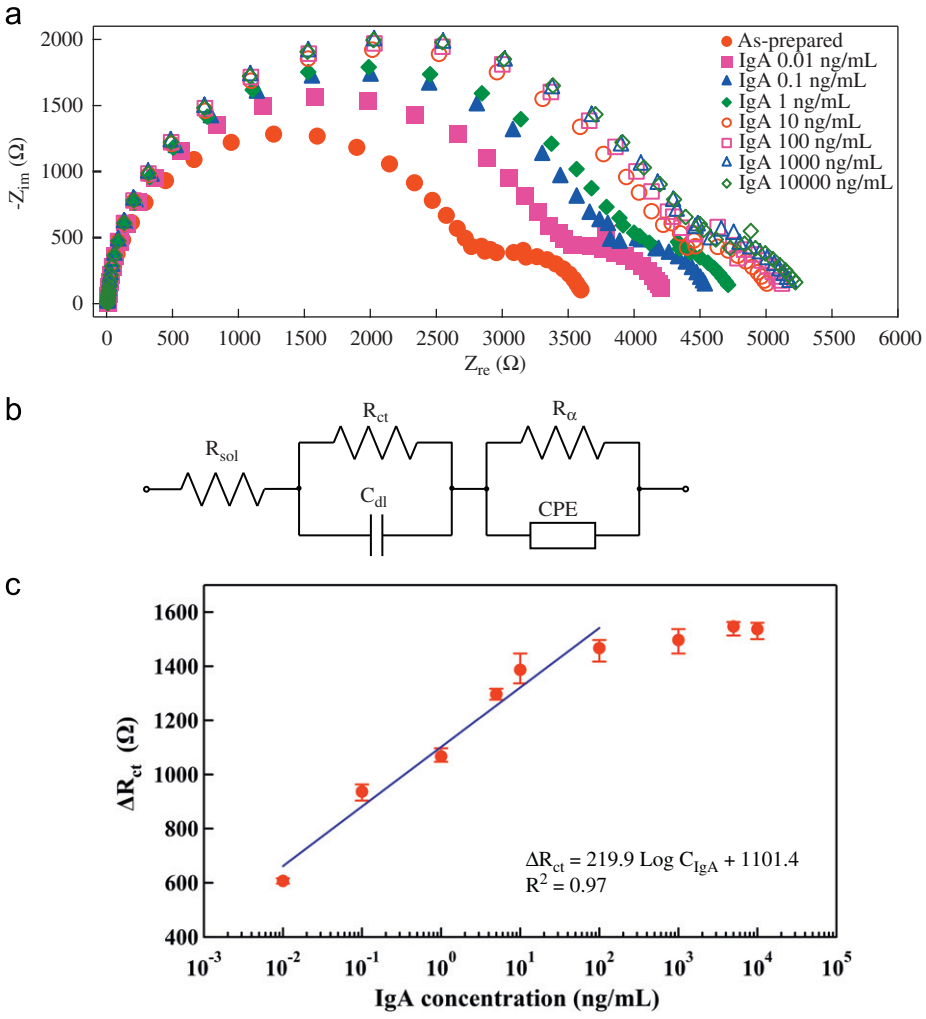

Fig. 1. (a) Nyquist plots of the impedance spectra of an anti-IgA modified interdigitated electrode (IDE) surface immersed in various concentrations of IgA, (b) An equivalent circuit model used in this study for analysis, (c) A calibration curve of the IgA immunosensor.

water. Next, the substrate was immersed into a 30 mM ethanolic solution of MPA for 16 h at room temperature to form a MPA-SAM on the IDE surface. The substrate was rinsed with ethanol and deionized water to remove any non-immobilized species and contaminants.

2.4. Immobilization of anti-IgA

To activate the carboxyl groups of the MPA, the SAM modified IDE was immersed in a solution containing 20 mg/mL of EDC and 10 mg/mL of NHS for 3 h at room temperature. After being washed with deionized water and dried with nitrogen gas, the sample was exposed to 250 μg/mL anti-IgA in PBS (pH 4) for 16 h at 4 °C. The usage of low pH PBS is intended to preserve the NHS ester activity (Hermanson, 2008). Following this procedure, anti-IgA molecules were immobilized on the IDE surface through a covalent bond formed between the amino group of anti-IgA and a corresponding carboxyl group of MPA. Subsequently, unbound anti-IgA was washed away using PBS (pH 4). Finally, the IDE was immersed in PBS (pH 4) containing 3% BSA for 3 h at room temperature to block the nonspecific binding sites and washed twice with PBS (pH 4) and deionized water.

2.5. Measurement and apparatus

To characterize the IgA sensor performance, the prepared sample was immersed in PBS (pH 6) containing different concentrations of IgA at 37 °C for 30 min and washed carefully twice with PBS (pH 6 and pH 7.4). EIS measurements were performed in PBS buffer (pH 7.4) containing a mixture of 2 mM $K_4[Fe(CN)_6]$, 2 mM $K_3[Fe(CN)_6]$ and 0.1 M KCl. The EIS spectra were recorded at an equilibrium potential without external biasing in the frequency range of $0.1-1\times10^5$ Hz with a 10 mV amplitude using an Autolab PGSTAT128N (Metrohm, Netherlands).

To observe the surface morphology of the samples, AFM experiments were performed in dynamic force mode under an air atmosphere using an SPM 9700 (Shimadzu, Japan) instrument.

3. Results and discussion

3.1. Performance of IgA sensor

For the characterization of the sensor performance, the successive cycles of the immersion in the fixed IgA solution and the corresponding EIS measurement were performed for each IgA concentration from the lowest to the highest concentration. The sensor was rinsed with deionized water after each measurement. Fig. 1a shows the Nyquist plots of the EIS spectra for the sample exposed to various IgA concentrations (0.01–10,000 ng/mL) together with the as-prepared sample (washed with pH 7.4 PBS before the measurement). It was observed that two semicircles appeared in each spectrum. As the IgA concentration was increased, the diameter of the semicircle appearing in the higher frequency range (the left semicircle in Fig. 1a) was increased. In general, the change in the semicircle diameter is a result of the change in the interfacial charge transfer resistance (R_{ct}); that is, the resistance corresponding to the carrier transfer from the modified electrode to the ferricyanide in the solution. Thus, the observed diameter increase is explained as the adsorption of IgA onto anti-IgA following an antigen–antibody reaction, where the adsorption of IgA effectively blocks the $[Fe(CN)_6]^{3-/4-}$ leading to an increase of R_{ct}. The increase of R_{ct} was observed in the concentration range of $0.01-100$ ng/mL. Over the IgA concentration of 100 ng/mL, no change in the diameter of the semicircle was observed, which indicates a constant R_{ct} value in the high concentrations of IgA. We consider that this behavior corresponds to the saturation of the anti-IgA binding sites.

3.2. Equivalent circuit analysis

To evaluate R_{ct}, the EIS results were simulated with an equivalent circuit as shown in Fig. 1b. Here, we assumed that the organic layer formed on the IDE (anti-IgA layer and SAM layer) was divided into two parts: the interfacial part and the inner part. The interfacial part was expressed by the parallel connection of R_{ct} and C_{dl} (the double layer capacitance), and the inner part was expressed by a constant resistance, R_{α}, and a constant phase element (CPE). The parameter R_{sol} represents the resistance of the bulk solution. Numerical fittings were performed for all the spectra. Then, we obtained all the parameters that reproduce well the experimental results (see Fig. S1 and Table S1, Supporting Information). Fig. 1c shows a calibration curve of the change in R_{ct} (ΔR_{ct}) vs. logarithmic IgA concentration, where ΔR_{ct} is calculated using the following equation: $\Delta R_{ct}=R_{ct}-R_{ct}$ (as-prepared). As seen in this figure, ΔR_{ct} linearly increases with increasing logarithmic IgA concentration in the 0.01–100 ng/mL range. Then, in much higher concentrations, ΔR_{ct} remained at a constant value. The well-defined linear dependence of ΔR_{ct} on the logarithmic IgA concentration demonstrates that the sample can be used as an IgA immunosensor. The observed detection limit of 0.01 ng/mL is the lowest recorded for an IgA immunosensor based on EIS (Chen et al., 2010). This behavior indicates that our approach of using an IDE with a simple surface is effective for the fabrication of a high performance immunosensor. Note, the calibration line can be slightly shifted between different samples,

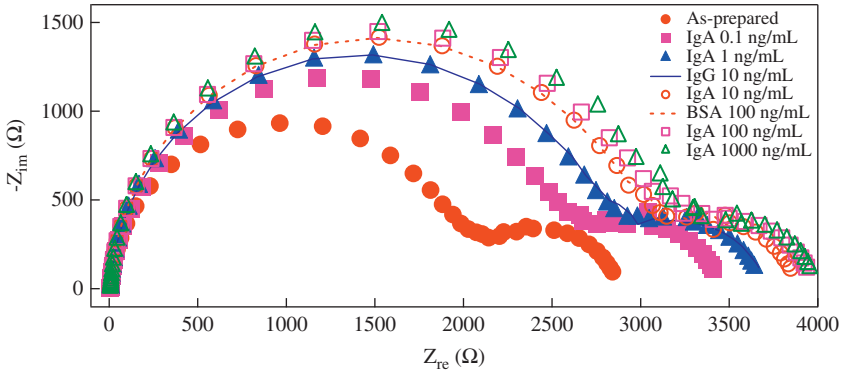

Fig. 2. Nyquist plots of the impedance spectra of anti-IgA modified IDEs interacted with different concentrations of IgA and IgG. The measurements were performed from the lowest to the highest IgA concentration. Between the measurements of 1 ng/mL and 10 ng/mL IgA, and between 10 ng/mL and 100 ng/mL, the sample was interacted with 10 ng/mL IgG solution and 100 ng/mL BSA solution, respectively.

however, the slope of the calibration line was fairly constant (see Fig. S2, Supporting Information).

3.3. Selectivity of IgA immunosensor

For practical applications, it is necessary to detect the IgA concentration selectively in samples that consist of a mixture of various proteins. To verify the selectivity, we examined the effects of both IgG and BSA on the EIS measurement. IgG has a similar protein structure to that of IgA, being present in human serum at a higher concentration than IgA. Thus, we investigated its interfering effect. BSA was also tested as a typical biological protein. A series of EIS measurements were performed for the IgA concentration range of 0.1–1000 ng/mL, from the lowest to the highest concentration. The sensor was rinsed with deionized water after each measurement. Between the measurements of 1 ng/mL and 10 ng/mL IgA, the sample was immersed into the IgG solution (10 ng/mL) for 30 min, and the EIS data were recorded to assess the impact of IgG exposure. In the same manner, the impact of BSA exposure (100 ng/mL) for 30 min was also examined between the measurement of 10 ng/mL and 100 ng/mL IgA. This series of measurements allows us to investigate the sensor response to IgG and BSA, verifying the IgA activity at the same time. The obtained Nyquist plots are shown in Fig. 2. As the sensor was immersed in IgA solutions, the diameter of the semicircle on the high frequency side was gradually increased in the same manner as discussed in the preceding section. However, it was observed that the diameter of the semicircle did not change as a result of the IgG immersion: the plots of 10 ng/mL IgG (solid line in Fig. 2) replicate exactly those plots taken just before recording 1 ng/mL IgA. For additional IgA (10 ng/mL), the EIS spectrum responded sensitively with increasing diameter of the semicircle, which indicated that the immunosensor retained its activity. The results showed that IgG exposure caused no effect on EIS. The same non-response behavior was also observed for BSA exposure. These results demonstrate that the IgA immunosensor has a high selectivity for IgA without being interfered by IgG or BSA.

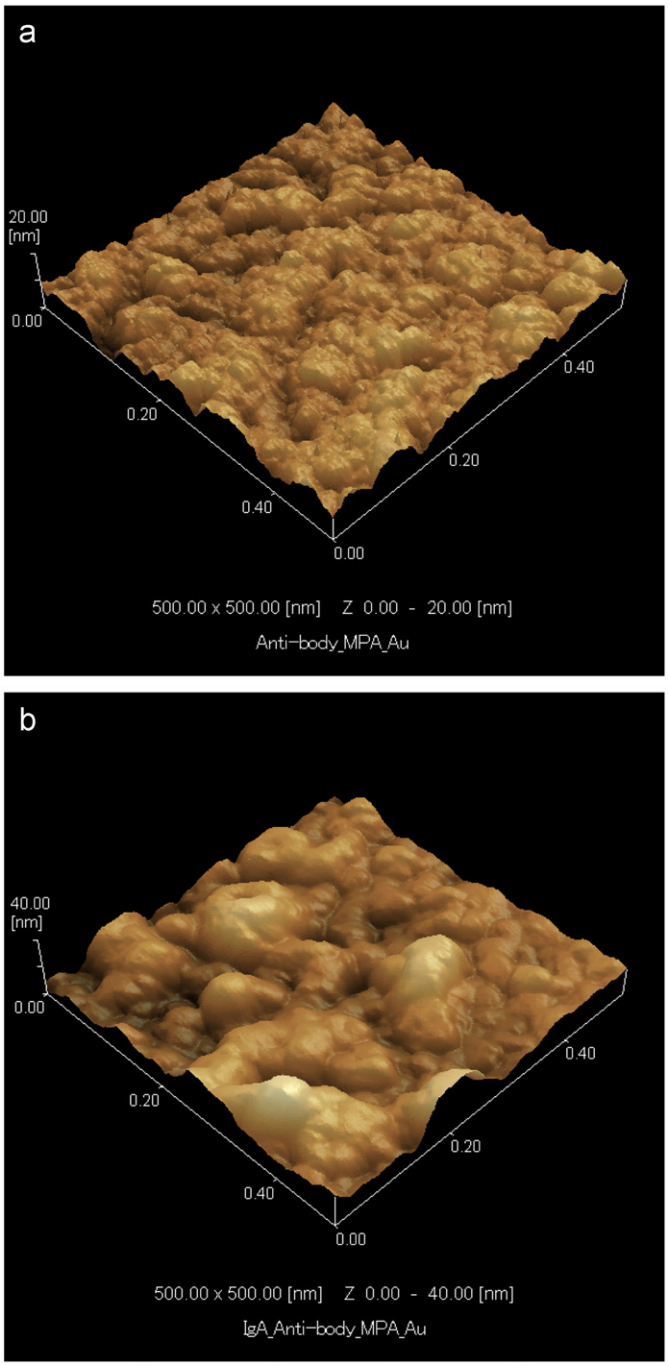

Fig. 3. AFM images (500 nm × 500 nm) taken before (a) and after (b) the IgA adsorption.

3.4. AFM measurement

To confirm the immobilization of IgA on anti-IgA, AFM measurements were carried out for the samples before and after the IgA adsorption. For the sample before IgA adsorption, a rough surface morphology corresponding to an aggregated pattern of anti-IgA was observed (Fig. 3a). After IgA adsorption, the surface became slightly smooth, containing many island structures (Fig. 3b). In this AFM image, we found that there were two types of island structure: small islands with sizes of 20–30 nm and large islands with sizes around ~100 nm. According to a previous report based on x-ray diffraction experiments, the size of the IgA dimer is 27 nm (Varshney and Li, 2009). Thus, the small islands will correspond to the IgA dimer adsorbed on the anti-IgA surface. For the large islands, we assume that these are IgA clusters in which several IgA dimers are bound together. From the above results, it was confirmed that IgA was certainly attached on the surface of anti-IgA.

4. Conclusions

To fabricate label-free IgA biosensors, we immobilized anti-IgA on the IDE surface of the immunosensor through the formation of covalent bonds with the carboxyl groups of an MPA SAM. The sensor exhibited linear behavior in the concentration range 0.01–100 ng/mL, which has the lowest detection limit among EIS based IgA biosensors studied. The immunosensor was found to have a high selectivity for IgA. AFM observation confirmed that the IgA had adsorbed on the anti-IgA surface. These results indicate that the combination of EIS and IDE with simple surface structure is practically effective in detecting antigen–antibody reactions for label-free biosensor applications.

Acknowledgments

This study was supported by KAKENHI (Grant-in-Aid for Scientific Research (B), 2136006) and the "Nanotechnology Network Project" of MEXT, Japan.

Appendix A. Supporting information

Supplementary data associated with this article can be found in the online version at http://dx.doi.org/10.1016/j.bios.2012.07.052.

References

Arya, S.K., Chornokur, G., Venugopal, M., Bhansali, S., 2010. Analyst 135, 1941–1946.
Bogomolova, A., Komarova, E., Reber, K., Gerasimov, T., Yavuz, O., Bhatt, S., Aldissi, M., 2009. Analytical Chemistry 81, 3944–3949.
Chen, X., Zhang, K., Zhou, J., Xuan, J., Yan, W., Jiang, L.P., Zhu, J.J., 2010. Biosensors and Bioelectronics 25, 1130–1136.
Daniels, J.S., Pourmand, N., 2007. Electroanalysis 19, 1239–1257.
Gosling, J.P., 1997. In: Price, C.P., Newman, D.J. (Eds.), Principles and Practice of Immunoassay, 2nd ed. Stockton, New York, pp. 349–388.
Hermanson, G.T., 2008. Bioconjugate Techniques, 2nd ed. Academic Press, Amsterdam.
Kutukculer, N., Karaca, N.E., Demircioglu, O., Aksu, G., 2007. Pediatric Allergy and Immunology 18, 167–173.
Laschi, S., Mascini, M., 2006. Medical Engineering & Physics 28, 934–943.
Lequin, R.M., 2005. Clinical Chemistry 51 (12), 2415–2418.
Li, H., Lee, S.J., Kraatz, H.-B., 2006. Analytical Chemistry 78, 6096–6101.
Lisdat, F., Schäfer, D., 2008. Analytical and Bioanalytical Chemistry 391, 1555–1567.
Niwa, O., Morita, M., Tabei, H., 1990. Analytical Chemistry 62, 447–452.
Qi, H., Wang, C., Cheng, N., 2010. Microchima Acta 170, 33–38.
Varshney, M., Li, Y., 2009. Biosensors and Bioelectronics 24, 2951–2960.
Wang, R., Wang, Y., Lassiter, K., Li, Y., Hargis, B., Tung, S., Berghman, L., Bottje, W., 2009. Talanta 79, 159–164.
Xu, D.K., Xu, D.W., Yu, X., Liu, Z., He, W., Ma, Z., 2005. Analytical Chemistry 77, 5107–5113.
Yang, L., Li, Y., Erf, G.F., 2004. Analytical Chemistry 76, 1107–1113.